IEEE Access
Multidisciplinary | Rapid Review | Open Access Journal

Received 11 April 2025, accepted 15 May 2025, date of publication 22 May 2025, date of current version 2 June 2025.

Digital Object Identifier 10.1109/ACCESS.2025.3572582

RESEARCH ARTICLE

A Prognostic Framework for Rotating Machines Considering Multi-Component Fault Scenarios

ADAM LYCKSAM[1,2], MATTIAS O'NILS[1], AND FAISAL Z. QURESHI[1,3], (Senior Member, IEEE)
[1]Department of Computer and Electrical Engineering, Mid Sweden University, 85170 Sundsvall, Sweden
[2]SCA, 85188 Sundsvall, Sweden
[3]Faculty of Science, University of Ontario Institute of Technology, Oshawa, ON L1G 0C5, Canada

Corresponding author: Adam Lycksam (adalun@miun.se)

This work was supported in part by The Knowledge Foundation within the Industrial Graduate School Smart Industry Sweden.

ABSTRACT The importance of preventing failures in rotating machines has led to extensive research on diagnosis and prognosis methods based on vibration data. To achieve a high generalizability for these solutions, they need to handle high discrepancies between the data used for developing the method and the data from the target machine, a lack of historical events from the target machine and multi-component fault scenarios. Currently, state-of-the-art research has successfully found solutions targeting the first two challenges. However, these almost exclusively focus on single-component fault scenarios, meaning it is unclear how a method should be constructed considering a multi-component system. Therefore, this study constructs a framework for multi-component fault scenarios called Rotating Machinery Prognostic Framework (RoMaP) that leverages the advancements in anomaly detection, fault diagnosis and RUL prediction based on vibration data. To evaluate the potential of RoMaP, an instance based on state-of-the-art research was implemented and compared to other methods based on alternative frameworks. The results show that the instance of RoMaP had the best performance across many scenarios expected in an industrial environment, suggesting that it is a suitable approach for monitoring the health of rotating machines.

INDEX TERMS Fault diagnosis, remaining useful life prediction, bearing, rotating machinery, predictive maintenance.

I. INTRODUCTION

Considering the importance of preventing rotating machines from failing, much research has been devoted to developing methods to identify faults and predict the Remaining Useful Life (RUL) of components using vibration data. Methods based on statistics, physics, and Machine Learning (ML), particularly Deep Learning (DL), have shown promising results [1], [2], [3]. Despite this, there exists a substantial challenge in constructing a general solution that can handle the high discrepancies of data across different machines and a lack of historical events from the machine targeted for monitoring [2], [4]. To manage these challenges, advances in, for example, methods based on transfer learning have become a prominent way of constructing robust methods with high generalizability without the need for labelled data from the target machine [5], [6]. Despite these efforts, there is a lack of consideration of a system-level perspective in the design of these methods, and the overwhelming majority of studies focus on a single component, such as a bearing, belt, shaft, or gearbox [3], [5], [7], [8]. This is a significant issue considering that vibrations from a machine in an industrial environment cannot be limited to the failure of a single component. Furthermore, considering the importance of accurate decision support for the user to make appropriate maintenance actions and the differences in severity and degradation time between faults, there is a necessity for methods to acknowledge different types of fault scenarios. In this context, the lack of research on multi-component faults is highly problematic, and it is currently unclear how a method should be developed for this scenario [3], [5]. Therefore, this study suggests Rotating Machinery Prognostic Framework (RoMaP), which utilizes the advancements in anomaly detection, fault diagnosis,

The associate editor coordinating the review of this manuscript and approving it for publication was Yiqi Liu.

and RUL prediction based on vibration data and can successfully handle multiple-component fault scenarios on a general basis. The framework is evaluated by implementing an instance in various scenarios expected in an industrial application and compared against the state-of-the-art. In summary, the novelty of this study is that it:

- Suggests a hybrid framework based on fault diagnosis, anomaly detection, and RUL prediction that can be used in a multi-component context for rotating machines using vibration data.
- Display the robustness of a method using the framework, considering multiple metrics across various tasks in a multi-component setting, expected in an industrial application.
- Demonstrate the importance of research from a system-level perspective by highlighting the limitations of current research based on single-component fault detection and RUL prediction.

An overview of the framework is displayed in Figure 1 and shows that models on an individual level are combined with general anomaly detection to form a system-level monitoring.

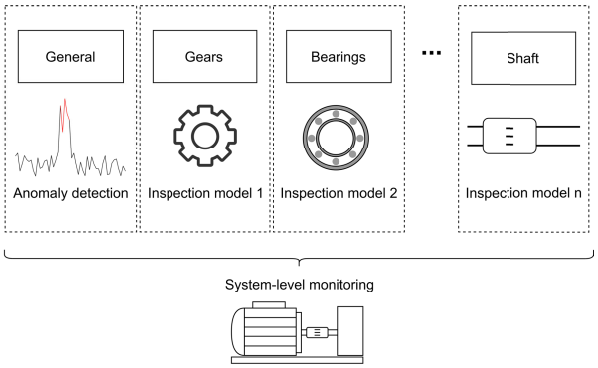

FIGURE 1. Overview of the suggested framework, which consists of component-level methods supported by a general anomaly detection.

II. BACKGROUND

Currently, most research on rotating machines for predictive and condition-based maintenance using vibration data focuses on either fault diagnosis or RUL prediction on components such as the shaft, gears, and bearings [5]. While diagnosis methods aim to notify the user of fault occurrences, methods based on RUL prediction notify the user when they need to take action. Concerning the latter, several different methods exist, and one of the main differences between approaches is the determination of the start of the degradation of the components' health. One of the methods used, for example, in [9] and [10], is based on the assumption that the RUL prediction starts when the component is commissioned. This means that the algorithm learns to consider both the normal state and the faulting state of the component. The challenge with these methods, as demonstrated in Figure 2, is that the time between normal operations varies significantly, making them seemingly challenging to apply in practice as a general solution.

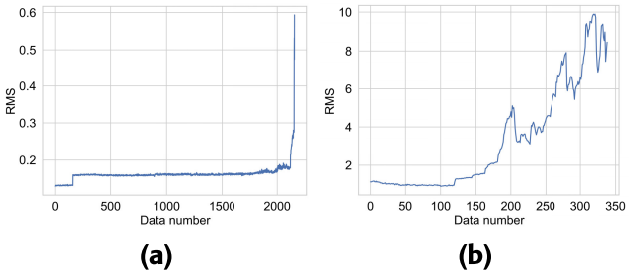

FIGURE 2. The RMS of bearing two different run-to-failure datasets.

To handle this, several studies, such as [11] and [12], estimate the First Prediction Time (FPT), sometimes referred to as Fault Occurrence Time (FOT) [13] or initial fault time [14], when an incipient fault in the component is predicted to start. From this point, a RUL prediction method, based on, for example, DL, is utilized to determine the component's end of life [14]. This procedure is theoretically beneficial because only the component's faulty state is considered, making it more generalizable. However, predicting FPT is not straightforward, and several different approaches exist. One method is based on creating a Health Indicator (HI) that can detect the FPT using anomaly detection. These ranges from simple statistical methods such as the Root Mean Square (RMS) or kurtosis of the raw signal [12], [13], [15], autoencoders based on DL [11], methods measuring the probabilty distribution distance based on the output of a Gaussian Mixture Model (GMM) [16], [17] to methods targeting the fault charactariscts of the component by considering the fault frequencies [18], [19], [20]. In addition, there exist methods such as [21] which use fault diagnosis based on DL to define FPT. Despite this, most studies consider a single-component scenario where bearing analyses are most common [5]. In addition, most benchmark datasets are from a laboratory environment where the impact of factors such as noise expected in the industrial setting can be reduced [3]. Because of this, it is unclear if these methods can handle noise or multi-component fault scenarios expected in industrial applications. One concern, for example, is that because these methods only separate between normal and faults from a single component, they take excessive consideration of factors such as the amplitude of the vibration signal and not the fault characteristics. This concern is supported by the fact that different mechanical faults are not easily separable without examining the fault characteristics. To exemplify this, Figures 3 show the raw time series signal and the RMS for two fault types from two components with no substantial difference in relative amplitude.

Therefore, it is essential to develop methods that handle high discrepancies in data and multi-component fault scenarios. Many types of solutions are worth exploring to achieve this. One is to consider end-to-end diagnosis and RUL prediction methods to detect the FPT and distinguish between degradation patterns in different fault scenarios, such as an extension to [21]. In this context, there exist studies

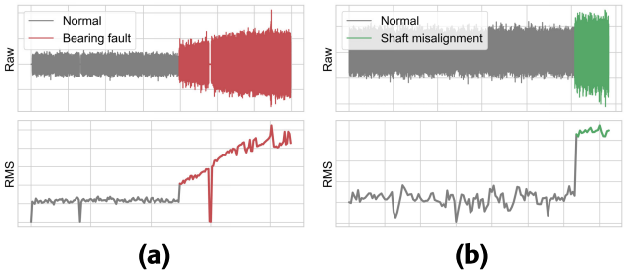

FIGURE 3. The raw vibration data and RMS from two different faults. (a) Bearing fault. (b) Shaft misalignment.

that for diagnosis tasks include different faulty components during training, such as [22] and [23], that considered bearings and gear faults using an end-to-end solution based on DL. However, these assume that fault samples from the machine targeted for monitoring are available during training, which is not necessarily true. In addition, the general challenge with these approaches is the open-world classification problem, where faults not considered during training might be present. In addition, when considering the variations of degradation and fault patterns across machines, this approach is challenging to apply as a general solution.

A second option, as encouraged by [1] and [24], is to develop HI methods for each component that can distinguish between other fault scenarios and then use prognosis methods to predict the RUL based on the indicator. However, designing indicators that do not react to fault scenarios other than what they are designed for is not easy, especially considering the variations in the data across machines.

To address the limitations of these approaches, this study suggests a hybrid framework that combines diagnosis and RUL prediction methods with anomaly detection. This approach allows the strengths of each method to be utilized to construct a reliable method that can effectively capture degradation and separate different fault scenarios.

III. FRAMEWORK

A summary of the proposed framework used for each vibration sensor separately is illustrated in Figure 4. The objective of the approach is to provide timely and informative alerts to the user regarding what type of maintenance is required and when it should be performed. To achieve this, separate models are developed for each component, focusing individually on fault diagnosis and RUL prediction. The reason for this is the complexity of building a method to cover all scenarios, considering the unique fault characteristics of each component. This setup also makes it easy to adjust or add a model for a new scenario without affecting the other.

Rather than relying on a single approach to predict faults and determine the start of health degradation, FPT, the solution integrates both diagnosis and anomaly detection in a hybrid framework. This combined strategy has been shown to offer substantial benefits, as supported by previous studies [5]. The anomaly detection is based on a general HI. This paper distinguishes between two types of HI methods: general and component-specific. A general HI method does not explicitly target the fault characteristics of any specific component and is developed to capture all fault scenarios. In contrast, a component-specific method is designed to detect and assess faults associated with a particular component, based on its unique vibration data signatures.

The following section will describe the different parts of the method in detail.

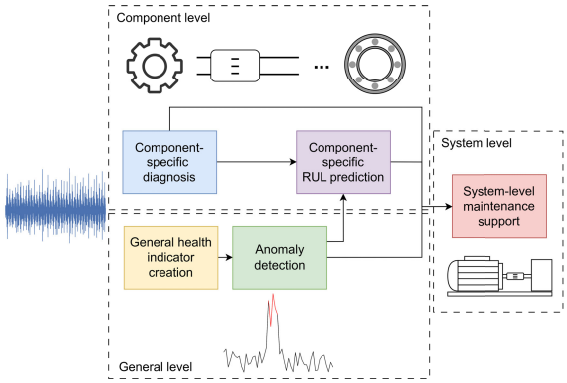

FIGURE 4. Overview of the different components of the suggested framework and their connection to each other.

A. COMPONENT FAULT DIAGNOSIS

For the fault diagnosis, each model is developed for a particular component in the machine. This means a single diagnosis model will include all fault scenarios for a particular component. For a bearing, this can, for example, include inner ring, outer ring, and rolling element fault scenarios. Each model must be developed based on the fault characteristics to separate it from other types of faults and predict healthy behaviour for any fault scenario on which it is not trained. This means that before a model is chosen, it needs to be validated against other faults. Lastly, the model must handle the varying operational conditions found across different machines, including differences in noise, sampling rate, rotational speed of the shaft, and component type. Such methods include [25], [26], [27].

B. GENERAL HEALTH INDICATOR AND ANOMALY DETECTION

Another important part of the framework is anomaly detection. This paper defines an anomaly as an abnormal event that is not necessarily a fault. This can be distinguished from fault diagnoses, which means ignoring abnormal events where the machine is healthy. The purpose of incorporating anomaly detection is to validate the diagnosis's prediction and identify faults not covered by any component-specific diagnosis model. This ensures that the system can be successfully deployed without needing a diagnosis model for all the components in the machine. The dependency on anomaly detection for unknown fault scenarios is lowered when more component-specific diagnosis methods are added to the framework. In the framework, an anomaly is triggered after a predefined number of consecutive HI values exceed

a threshold. The HI can be derived using any method, but it is crucial that it can separate all fault scenarios from data describing a healthy machine. Since it is suggested to be used as input for the RUL prediction, it is also essential to have a high level of monotonicity, consistency, and robustness as highlighted in [14]. Based on this criterion, an example of a suitable alternative is the autoencoder suggested in [11].

C. COMPONENT RUL PREDICTION

Similarly to component fault diagnosis, each component gets its own model for RUL prediction. This is because the development time and the degradation pattern may significantly differ between the faults in different components. To ensure that there is a fault and that degradation is triggered, this model will start to predict once an anomaly and a fault for that component are detected. This study suggests that the model uses the general HI as input for RUL prediction, but can also use a component-specific HI or raw data. Regardless of data input, the model must be validated on cross-machine scenarios, as expected in industrial applications.

D. PROCEDURE

Figure 5 presents an example of the procedure. In this example, the user is notified of a bearing degradation at point FPT, where the bearing diagnosis method has found a fault, and an anomaly is detected. Then, the RUL prognosis method will use the RUL Prediction Time (RPT) as the initial point of the degradation. This is the last point before the FPT, when a HI point is above the anomaly threshold. This point is used instead of FPT because the diagnosis method will sometimes not detect the fault directly, making it challenging to construct an accurate RUL prediction method. Then the RUL prediction method outputs the health status of the bearing, which in this example means mapping the HI to a value from 1, which is healthy, to 0, when the bearing is expected to fail.

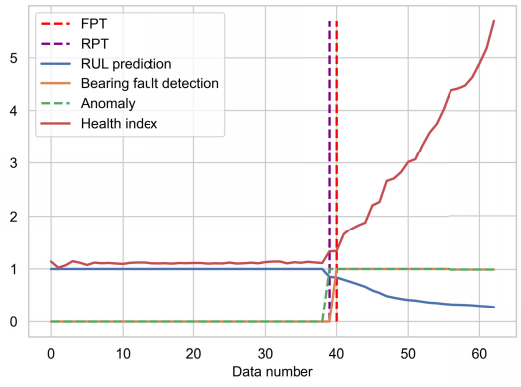

FIGURE 5. An example of the procedure using the framework. FPT is when a fault is predicted and occurs when a component-specific fault and an anomaly are detected. RPT is the RUL prediction model's initial prediction time, which maps the HI from 1 (healthy) to 0 (failure).

E. SYSTEM-LEVEL MAINTENANCE SUPPORT

Given the combined system, the user will be able to get information based on the following scenarios: (1) a fault is detected in one or more components, there is an anomaly, and a prediction of RUL (2) a fault is detected in one or more components, and there is no anomaly detected, and (3) there is no fault detected, but there is an anomaly detected. These are explained below.

1) SCENARIO 1

In scenario 1, the user is given information about the fault, what caused it, and the RUL of that component. This means that the user can plan maintenance actions before failure is expected.

2) SCENARIO 2

In scenario 2, the user is not given a prediction because the severity is not above the anomaly threshold. This can still mean that the diagnosis is correct, but the user does not need to take any action for the foreseeable future.

3) SCENARIO 3

Scenario 3 means an anomaly has been detected without a fault being detected in any component. In this scenario, the user is expected to examine the machine's health and look for anomalies physically. Despite not going into exactly what caused the fault based on the vibration data, the system will still be able to rule out the fault scenarios that are being monitored. In this way, the user can understand what to look for in the physical inspection.

IV. CASE STUDY

A case study was conducted to evaluate an instance of the suggested framework and, based on this, demonstrate its potential effectiveness. To simulate scenarios expected in an industrial application, the following aspects were considered: no historical faults from the target domain, deployment on a new machine not part of the training, and the occurrence of faults from multiple components. The experiment evaluates the scenario where component-specific methods for bearing faults are developed and other fault scenarios, including shaft misalignment, imbalance, and looseness, for which no component-level method exists.

A. DIAGNOSIS METHOD

In the case study, ConnKIDDG suggested in [25] was used for bearing fault diagnosis. Because this study focuses on the framework and its usability, it is not restricted to the method, and the implementation details are referred to in the original paper. A similar setup as was used in [25] is applied in this study. All parameters used in training were consistent throughout the experiment, and only the normal health state of the target machine was used during training.

B. RUL PREDICTION

Bidirectional Long-Short-Time-Memory (Bi-LSTM) was chosen for the RUL prediction, which considers both the forward and backward directions of a sequence. This method is applied with promising results in state-of-the-art research

such as [11]. In the experiment, common among previous work [14], the algorithm's optimization objective was to map the HI to the component's degradation. Each input consisted of a window of the past 10 HI values, and the model comprised one Bi-LSTM layer with eight units and a fully connected layer that outputs the mapping value.

C. GENERAL HEALTH INDICATOR AND ANOMALY DETECTION

For the general HI, a Convolutional Autoencoder (CAE) was used to learn from windows of 600 data points from the raw vibration data. These samples were taken from the first 25% (if no fault was observed before that time) of the different tasks since this was assumed to be a healthy state. The HI was constructed by taking the mean error of the reconstructed output and the actual output. The model consisted of two layers for the encoder with ReLU as activation, a kernel size of 3, a stride length of 2, and 32 and 64 filters, respectively. The decoder used three transposed convolutional layers, the first two using ReLU as activation, the same kernel size as the encoder, and 64, 32, and 1 filters.

D. DATASESTS

The experiment considered four publicly available datasets from different machines and operational settings to simulate the variations expected in the industrial environment. The datasets used were the XJTU-SY bearing run-to-failure dataset, the SCA bearing dataset, the IMS bearing run-to-failure dataset, and the University of South Korea multi-component fault dataset.

1) XJTU-SY

The XJTU-SY bearing run-to-failure dataset [28] includes 15 different run-to-failure scenarios from a laboratory environment with three operational settings. In the experiment, all scenarios except the fourth case in condition one (12kN load and 35Hz rotational speed of the shaft), the third case in condition two (11kN load and 37.5Hz rotational speed of the shaft) and the first and fifth case from condition three (10kN load and 40Hz rotational speed of the shaft) were used. These were excluded because they include a limited amount of healthy data or faults other than inner, outer, or rolling element faults, which were not considered in the case study.

2) IMS

The IMS run-to-failure bearing dataset [29] consists of readings from different sensor positions with the same operational condition in all scenarios from a laboratory environment. In the case study, the third sensor on the first test and the first sensor on the second test were used.

3) SCA BEARING DATASET

The SCA bearing dataset [4], [30] consists of 11 scenarios from different machines in an industrial environment with various operational settings. Of the 11 scenarios, 10 are bearing faults with outer ring, outer ring and rolling element faults, and 1 is a shaft misalignment fault. This dataset was used despite not being a run-to-failure dataset due to the importance, as also argued in [5], of evaluating on data from the industrial environment.

4) UNIVERSITY OF SOUTH KOREA

The dataset, in this paper defined as US [31], includes a variety of fault scenarios from different components, including bearing faults, looseness, shaft misalignment, and shaft imbalance from a laboratory environment. It also includes different operational settings and bearing types. In the case study, the scenario with bearing 30204, the rotational speed of 1600 RPM, and the scenarios with the highest severity of shaft misalignment, shaft imbalance, and looseness were used.

5) DATASETS USED FOR DEVELOPING DIAGNOSIS MODEL

Because the paper's main contribution is the framework and to streamline the paper, the diagnosis datasets used in the training of ConKIDDG are not listed. These are described in detail in the original paper [25].

E. CASES

Three different types of scenarios were considered in the case study. The first was bearing RUL tasks from the laboratory environment listed in Table 1. Similar to previous work such as [10] and [11], the labelling was determined as linear degradation from FPT (or RPT for RoMaP) to the component failure. Only healthy data from the target domain were allowed for training. In the tasks with the XJTU-SY dataset, faults from other operational conditions from the same dataset and IMS were used for training. In the IMS tasks, only faulty data from XJTU-SY were used for training. The second scenario was bearing fault detection from the industrial environment with the tasks listed in 2. Because these are not RUL scenarios, fault detection was only considered. The third scenario was non-bearing related faults listed in Table 3.

F. COMPARISON

To evaluate the potential of the suggested method, a comparison based on alternatives other than the suggested framework was conducted. Based on previous work, three other architectures were considered: General Indicator Framework (GIF), Specific Indicator Framework (SIF), and General Specific Indicator Framework (GSIF). GIF, displayed in Figure 6a, was used because it is one of the most common approaches to determine the FPT in current research [14]. In this scenario, a general HI was constructed to determine the FPT and predict the RUL. Two methods were used: the CAE described in section IV-B and RMS.

The framework SIF is shown in Figure 6b, where a general HI is used for faults that the component-specific HI does not cover, and the component-specific HI is used to determine the FPT for the RUL prediction. The purpose of testing this framework was to examine the potential of

TABLE 1. Tasks for bearing run-to-failure from the laboratory environment.

Tasks	Domain	Deployment	Fault scenario
1-1, 1-2, 1-3, 1-4	XJTU-SY setting 1	Cross operations	Inner and outer ring bearing fault
1-5, 1-6, 1-7, 1-8	XJTU-SY setting 2	Cross operations	Inner and outer ring bearing fault
1-9, 1-10, 1-11	XJTU-SY setting 3	Cross operations	Inner and outer ring bearing fault
1-12	IMS scenario 1 position 3	Cross machine	Inner ring bearing fault
1-13	IMS scenario 2 position 1	Cross machine	Outer ring bearing fault

TABLE 2. Tasks from the industrial environment where the bearing was changed before failure.

Tasks	Domain	Deployment	Fault scenario
2-1, 2-2, 2-3, 2-4, 2-5, 2-6, 2-7, 2-8, 2-9, 2-10	SCA bearing faults	Cross machine	Inner, outer and rolling element bearing fault

TABLE 3. Tasks with non-bearing related mechanical faults.

Tasks	Domain	Deployment	Fault scenario
3-1	SCA task 11	Cross machine	Shaft misalignment
3-2	US scenario 3 setting 3	Cross machine	Shaft misalignment
3-3	US scenario 3 setting 3	Cross machine	Imbalance
3-4	US scenario 3 setting 3	Cross machine	Loosness

only using component-specific HI methods as encouraged by [1] and [24], and thereby removing the need for a diagnosis model.

Lastly, SGIF, shown in Figure 6c, is similar to SIF but uses the same validation procedure as in RoMaP, meaning that the FPT was determined both by considering the general HI and the specific HI. Consequently, if the general HI identifies an anomaly, a single value from the component-specific HI above the threshold denotes the FPT. The component-specific HI, which is defined as Frequency RMS (FRMS), was used. It uses the RMS of the spans of the fault frequencies of the bearing with a 2% error margin, considering 3 harmonics. This type of method was used by previous work, such as [18], with promising results. Both the squared enveloped spectrum and the non-squared enveloped spectrum were considered.

All compared methods used the RUL prediction method described in section IV-A. In addition, for all instances based on SIF and SGIF, the CAE described in IV-B was used.

V. SETUP

To handle the variation in amplitude across domains, all HI values were normalized so that the first 25% of the data,

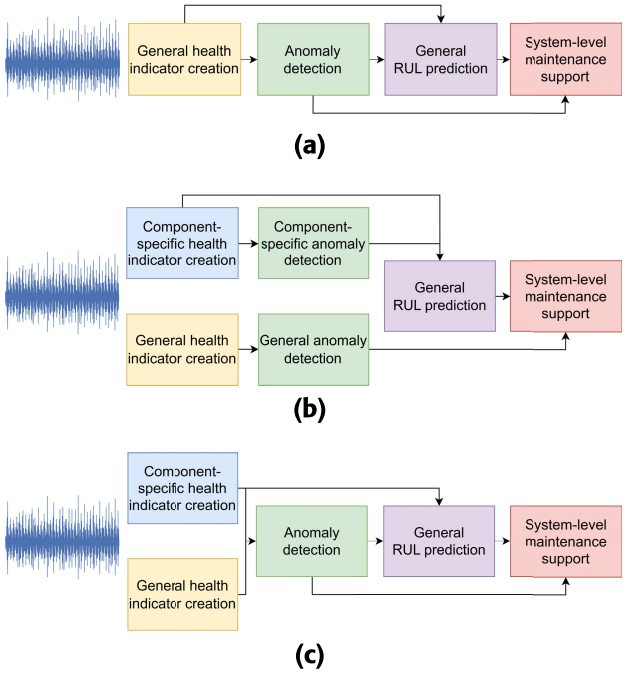

FIGURE 6. Bearing degradation prediction using different methods for task 1-11. (a) GIF. (b) SIF. (c) SGIF.

which was assumed to be normal, had a mean of 1. This data was also excluded from the test data. Concerning the threshold for the different HI methods, these were set to $x\sigma$ where σ is the standard deviation of the normalized first 25%, and x is a multiple set to 3 as default, similar to previous work [16]. In addition, to reduce the effect of noise, it was assumed that a point is anomalous, considering both the general and the component-specific (except for SGIF) HI if three of the four past points were anomalous. To reduce the influence of fluctuation in the HI for the prediction of the RUL, the indicators were processed using a window of the mean values from the previous 10 values, which was carried out after the FPT was determined.

All models were trained using a fixed learning rate of 0.001 using Adam as optimizer. The CAE was trained for 150 epochs using Mean Squared Error Loss (MSE) as optimization metric, Bi-LSTM for 50 epochs using MSE, and ConKIDDG, the same as in the original paper [25].

VI. METRICS

The experiment results were measured using three different metrics. The first was Root Mean Squared Error (RMSE), which was used to compare against the ground truth degradation:

$$RMSE = \sqrt{\sum_{i=1}^{n} \frac{(y_i - \hat{y}_i)^2}{n}}, \tag{1}$$

where $\hat{y}_i$ is the predicted RUL value and y_i is the actual.

The second was the number of False Positives (FP), which determines the number of false alarms for the end user, namely faults detected before the ground truth, Fault Actual

TABLE 4. Performance on bearing RUL dataset of the compared methods with different metrics. Lower values for each metric are better.

Metric	Method	1-1	1-2	1-3	1-4	1-5	1-6	1-7	1-8	1-9	1-10	1-11	1-12	1-13	Avg
FP	GIF_{RMS}	0	0	0	3	0	0	33	0	64	0	0	0	0	7.69±18.45
	GIF_{CAE}	4	0	0	0	0	0	0	0	5	0	0	368	0	29±97.87
	SIF_{FRMS}	0	0	0	7	0	0	0	0	2251	28	0	207	0	189.62±597.59
	SIF_{F^2RMS}	0	0	0	15	0	0	23	2	2501	0	0	877	0	262.92±686.47
	$SGIF_{FRMS}$	0	0	0	3	0	0	0	0	52	0	0	189	0	18.77±51.03
	$RoMaP_{ConKIDDG}$ (our)	0	0	0	0	0	0	0	0	0	0	0	0	0	**0±0**
FATD	GIF_{RMS}	6	7	2	0	2	2	0	4	0	8	2	99	2	10.31±25.73
	GIF_{CAE}	0	8	15	0	2	4	2	10	0	10	1	0	65	9±16.84
	SIF_{FRMS}	4	2	2	0	2	2	2	2	0	0	2	0	2	**2.0±1.57**
	SIF_{F^2RMS}	2	2	2	0	2	2	0	0	0	6	2	0	2	1.54±1.60
	$SGIF_{FRMS}$	7	4	12	0	0	0	0	6	0	6	0	0	41	5.85±10.8
	$RoMaP_{ConKIDDG}$ (our)	7	5	16	2	4	4	1	4	14	9	2	126	25	16.85±32.2
RMSE	GIF_{RMS}	0.18	0.15	0.22	0.30	0.20	0.29	0.18	0.28	0.18	0.16	0.16	0.35	0.27	0.22±0.06
	GIF_{CAE}	0.21	0.13	0.20	0.31	0.07	0.33	0.17	0.12	0.07	0.21	0.08	0.34	0.17	0.19±0.09
	SIF_{FRMS}	0.10	0.15	0.25	0.49	0.08	0.28	0.13	0.28	0.39	0.16	0.11	0.42	0.31	0.24±0.13
	SIF_{F^2RMS}	0.11	0.19	0.18	0.41	0.18	0.25	0.17	0.19	0.41	0.20	0.09	0.46	0.22	0.24±0.11
	$SGIF_{FRMS}$	0.13	0.15	0.25	0.47	0.08	0.29	0.12	0.30	0.12	0.16	0.10	0.44	0.32	0.22±0.13
	$RoMaP_{ConKIDDG}$ (our)	0.17	0.13	0.28	0.29	0.07	0.21	0.14	0.13	0.09	0.16	0.11	0.19	0.15	**0.16±0.07**

Time (FAT). Since the RUL datasets do not provide the FAT, this was manually estimated using the squared enveloped frequency spectrum, a method commonly used by previous research such as [32].

In addition, the Fault Actual Time Delay (FATD) was the third metric used to capture the delay from the fault being apparent to the method's prediction of the fault. If a method identifies the fault before FAT, the metric is set to 0. This metric was not used for non-bearing-related fault scenarios.

Lastly, Missed Faults (MF) count the number of misclassified segments, which is defined as the fault scenario in each task. This means that if there is a bearing fault, the metric will count 1 if the method does not detect the fault (regardless of whether the anomaly detection method detects an anomaly). In addition, if there is no bearing fault and no anomaly is detected or a bearing fault is predicted, the metric will also count 1.

VII. RESULTS AND ANALYSIS

The results considering the bearing scenarios are presented in Table 4 and 5, and the non-bearing related scenarios in Table 6. Each instance is identified by a unique method in the implementation defined in subscript. For example, GIF_{CAE} means the framework GIF using a CAE for HI creation. Overall, the method based on the suggested framework $RoMaP_{ConKIDDG}$ had the highest accuracy across all metrics, apart from FATD, where it performed slightly worse for some tasks. An in-depth analysis of the result is presented in the following sections.

A. BEARING FAULT SCENARIOS

In the first scenario, where bearing faults were considered, all different degradation scenarios were correctly identified for all considered methods. It is observable that $RoMaP_{ConKIDDG}$ had the highest RUL prediction accuracy. A primary reason for this is that the method can detect a more suitable FPT. This is supported by the number of FP when not using $RoMaP_{ConKIDDG}$ and exemplified for tasks 1-9 using SIF_{FRMS} as comparison, shown in Figure 7. It can be seen that the approximation of FPT is early when the methods based on GIF, SIF, and SGIF were used, causing a large amount of FP and a poor prediction of the degradation for both the run-to-failure datasets and the industrial dataset. In contrast, when using $RoMaP_{ConKIDDG}$, the selection of FPT (and RPT) is shown to be more stable and accurate in relation to FAT. However, as expected, because of the stricter validation, there is sometimes a delay between the sign of a fault and the detection using $RoMaP_{ConKIDDG}$, which was higher than the other methods on the bearing run-to-failure scenarios but not in the industrial scenarios.

B. NON-BEARING RELATED FAULTS

A substantial difference between $RoMaP_{ConKIDDG}$ and the compared methods can be observed when considering faults unrelated to the bearing. When methods based on GIF, SIF, and SGIF were used, several MF were generated, which created a large amount of FP. In contrast, $RoMaP_{ConKIDDG}$ correctly identified all tasks as anomalies. The results underline the difficulty of using frameworks based on a component-specific HI to find the FPT. Figures 8, 9, and 10 display the performance using SIF_{FRMS}, SIF_{F^2RMS}, and the suggested approach $RoMaP_{ConKIDDG}$, which shows that both of the methods based on using a component-specific HI incorrectly identified a bearing fault. This means that the user will be told that there is a bearing fault and that the user can wait to take maintenance actions based on the RUL prediction, which might be highly inappropriate. In contrast, when using $RoMaP_{ConKIDDG}$, the user would be told that there is no bearing fault and to examine

TABLE 5. Performance of the industrial dataset with bearing faults compared methods with different metrics. Lower values for each metric are better.

Metric	Method	2-1	2-2	2-3	2-4	2-5	2-6	2-7	2-8	2-9	2-10	Avg
FP	GIF_{RMS}	0	0	0	10	120	0	0	0	0	0	13±35.79
	GIF_{CAE}	0	0	0	10	120	0	0	100	0	0	23±43.83
	SIF_{FRMS}	0	0	0	0	120	0	0	192	0	0	31.20±64.44
	SIF_{F^2RMS}	0	0	0	0	120	0	236	205	0	0	56.10±89.8
	$SGIF_{FRMS}$	0	0	0	10	124	0	0	0	0	0	13.40±36.99
	$RoMaP_{ConKIDDG}$ (our)	0	0	0	0	0	0	0	0	0	0	**0**
FATD	GIF_{RMS}	99	4	10	0	0	127	5	4	98	138	48.50±55.87
	GIF_{CAE}	4	4	1	0	0	115	4	0	99	4	**23.1±42.14**
	SIF_{FRMS}	4	8	25	13	0	115	4	0	97	78	34.40±42.16
	SIF_{F^2RMS}	4	4	38	9	0	39	0	0	98	74	26.60±33.29
	$SGIF_{FRMS}$	0	6	22	0	0	113	2	2	95	70	31.0±41.97
	$RoMaP_{ConKIDDG}$ (our)	0	0	29	7	5	75	4	3	60	60	24.3±28.04

TABLE 6. Performance of the non-bearing related mechanical faults compared methods with different metrics. Lower values for each metric are better.

Metric	Method	3-1	3-2	3-3	3-4	Avg/Sum
FP	GIF_{RMS}	14	57	50	57	44.50±17.84
	GIF_{CAE}	14	57	56	57	46±18.48
	SIF_{FRMS}	0	43	0	1	11.0±18.48
	SIF_{F^2RMS}	0	55	0	54	27.25±27.25
	$SGIF_{FRMS}$	0	55	0	61	29.0±29.08
	$RoMaP_{ConKIDDG}$ (our)	0	0	0	0	**0**
MF	GIF_{RMS}	1	1	1	1	4
	GIF_{CAE}	1	1	1	1	4
	SIF_{FRMS}	0	1	0	1	2
	SIF_{F^2RMS}	0	1	0	1	2
	$SGIF_{FRMS}$	0	1	0	1	2
	$RoMaP_{ConKIDDG}$ (our)	0	0	0	0	**0**

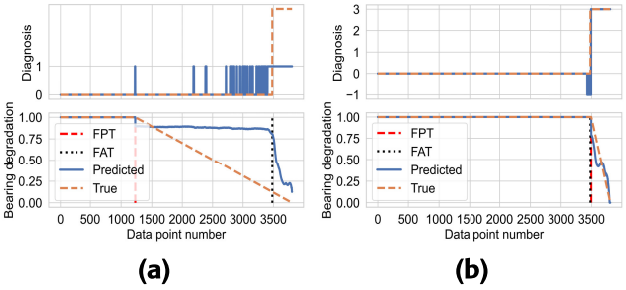

FIGURE 7. Bearing degradation prediction using different methods for task 1-9. (a) SIF_{FRMS}. (b) $RoMaP_{ConKIDDG}$ (our).

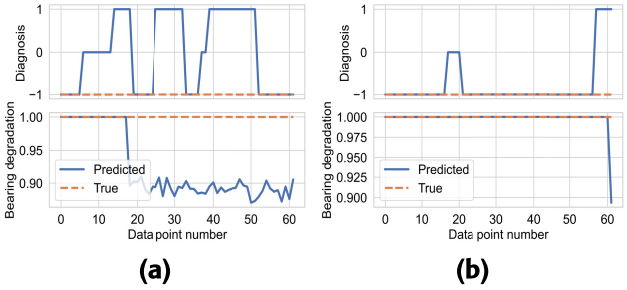

FIGURE 8. Bearing degradation prediction using SIF_{FRMS} for two cases of non-bearing fault. In the diagnosis, -1 means that the method has identified an anomaly, 0 means that the machine is healthy, and 1 means a bearing fault. (a) Task 3-2 shaft misalignment. (b) Task 3-4 looseness.

the machine, which increases the possibility of an appropriate maintenance action.

C. SENSITIVITY OF FPT

The sensitivity was also evaluated considering the determination of FPT and general anomaly detection by varying thresholds for the HI methods. The reason why this is particularly relevant is that the optimal threshold values are unknown in practice. For a method to be generally applicable, it must be robust against slightly suboptimal threshold values. Table 7 shows the average accuracy using different thresholds based on the standard deviation of the best-performing methods from Tables 4-6. As can be seen, the performance across all metrics is highly dependent on an optimal threshold for GIF_{CAE}, SIF_{FRMS}, and $SGIF_{FRMS}$. When a low threshold was used, FP, RMSE, and MF increased, and when a high threshold was used, FATD and MF increased. This means that a tradeoff exists between these metrics to reach the optimum, which will vary between different tasks and, therefore, becomes highly problematic in practice. In contrast, $RoMaP_{ConKIDDG}$ showed high robustness for different threshold settings. It displayed the highest performance across all metrics except for FATD, where it generally detected faults slightly later than the other methods for all thresholds. Only for a threshold value of 5σ can a notable decrease in performance be observed because the anomaly detection method missed

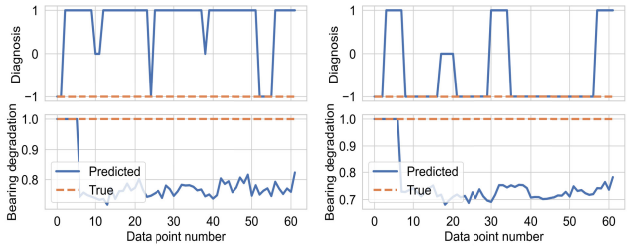

FIGURE 9. Bearing degradation prediction using SIF_{F^2RMS} for two cases of non-bearing fault. In the diagnosis, -1 means that the method has identified an anomaly, 0 means that the machine is healthy, and 1 means a bearing fault. (a) Task 3-2 shaft misalignment. (b) Task 3-4 looseness.

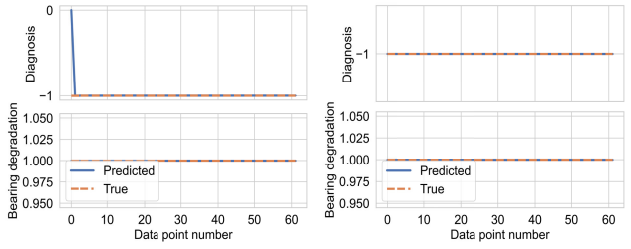

FIGURE 10. Bearing degradation prediction using the suggested method $RoMaP_{ConKIDDG}$ for two cases of non-bearing fault. In the diagnosis, -1 means that the method has identified an anomaly, 0 means that the machine is healthy, and 1, 2, and 3 are outer ring, rolling element, and outer ring faults, respectively. (a) Task 3-2 shaft misalignment. (b) Task 3-4 looseness.

TABLE 7. Performance of the compared methods with different thresholds for anomaly detection.

Metric	Method	1σ	2σ	3σ	4σ	5σ
FP	GIF_{CAE}	245.04	58.00	29.30	11.89	9.78
	SIF_{FRMS}	256.04	177.07	112.84	42.52	15.87
	$SGIF_{FRMS}$	87.44	44.00	18.30	13.15	9.52
	$RoMaP_{ConKIDDG}$ (our)	**0**	**0**	**0**	**0**	**0**
FATD	GIF_{CAE}	**4.19**	**8.65**	**15.13**	18.87	**21.22**
	SIF_{FRMS}	6.74	11.22	16.09	19.74	22.48
	$SGIF_{FRMS}$	12.17	13.13	16.78	**18.83**	22.91
	$RoMaP_{ConKIDDG}$ (our)	14.70	19.48	20.09	23.91	25.91
RMSE	GIF_{CAE}	0.24	**0.17**	0.19	0.22	0.17
	SIF_{FRMS}	0.27	0.23	0.24	0.23	0.22
	$SGIF_{FRMS}$	0.24	0.24	0.23	0.22	0.22
	$RoMaP_{ConKIDDG}$ (our)	**0.19**	0.20	**0.16**	**0.17**	**0.17**
MF	GIF_{CAE}	4	4	4	4	4
	SIF_{FRMS}	3	3	2	**0**	2
	$SGIF_{FRMS}$	3	3	2	2	3
	$RoMaP_{ConKIDDG}$ (our)	**0**	**0**	**0**	**0**	**1**

a non-bearing related fault scenario and generated a MF. The reason why $RoMaP_{ConKIDDG}$ consistently outperformed the other methods likely lies in the intelligence of the diagnosis method, which can handle more complex scenarios than the frameworks based on FRMS. Since the diagnosis method can be less reliant on the amplitude of the vibration signal than FRMS, it can handle variations in the signal more robustly. One example is task 1-7 shown in Figure 11, where the difference between using 2σ and 3σ is substantial. However, no performance difference is observed when using $RoMaP_{ConKIDDG}$, displayed in Figure 12.

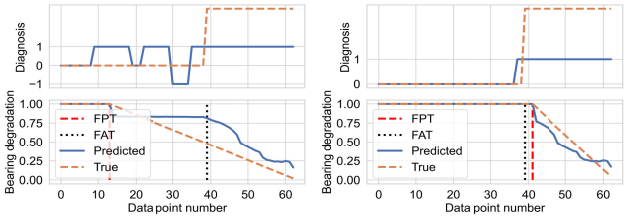

FIGURE 11. Bearing degradation for the task 1-7 task using different thresholds based on SIF_{FRMS}. (a) Two times the standard deviation. (b) Three times the standard deviation.

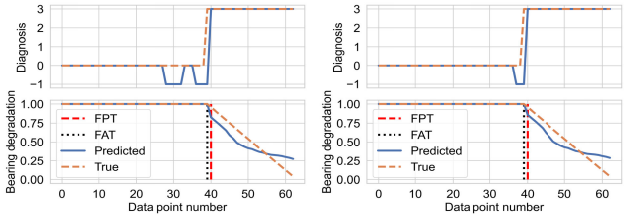

FIGURE 12. Bearing degradation for the task 1-7 task using different thresholds based on the suggested method $RoMaP_{ConKIDDG}$. (a) Two times the standard deviation. (b) Three times the standard deviation.

D. SENSITIVITY OF DIAGNOSIS

It is also valuable to display the advantage of combining general anomaly detection and fault diagnosis when determining the FPT. The risk when using only a fault diagnosis model to determine a fault is FP, since no single model is completely accurate. An example displayed in Figure 13 is the SCA dataset task 2-8, where the diagnosis model incorrectly predicted an inner ring fault when the bearing is healthy. However, because no anomaly is found, the user can be informed that they do not need to take action. The same type of output is observable when using $SGIF_{FRMS}$, but, as seen in the result, Table 7, it is not as robust as $RoMaP_{ConKIDDG}$ because of a less accurate diagnosis.

VIII. FINDINGS AND IMPLICATION

A summary of the performance of the different methods for multi-component fault diagnosis and RUL prediction is shown in Table 8. It can be used as a high-level general guideline for using the different frameworks. However, it is important to consider that the performance of each framework is highly dependent on which type of methods are used.

The result shows, as expected, that GIF_{CAE} and GIF_{RMS} are likely to fail in practical applications, and their use is limited to laboratory scenarios. This is because they are unable to separate different fault scenarios, as can be seen in Table 6. This is particularly interesting because a vast amount of research uses this approach to determine the

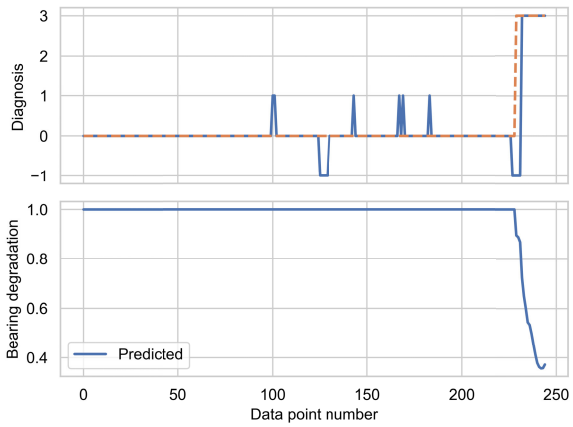

FIGURE 13. Sensitivity of diagnosis using RoMaP$_{ConKIDDG}$. In the diagnosis, -1 means that the method has identified an anomaly, 0 means that the machine is healthy, and 1, 2, and 3 are outer ring, rolling element, and outer ring faults, respectively.

FTP [14]. Instead, suitable approaches are instances based on frameworks like GIF$_{FRMS}$, GSIF$_{FRMS}$, and the suggested approach RoMaP$_{ConKIDDG}$, each of which has its advantages and disadvantages. The primary issue with using instances of GSIF and GIF is the reliance on thresholds, which, based on the result (Table 7), are challenging to set. Consequently, the risk is high FP when the threshold is too low, and a high FATD with the risk of missing fault scenarios when using a high threshold. In contrast, the result based on RoMaP$_{ConKIDDG}$ shows that it can be less dependent on an optimized threshold to deliver accurate user support, which results in high and consistent performance. It can also separate different fault scenarios, which, as indicated by the result, can be more challenging to achieve when using GSIF$_{FRMS}$ or SIF$_{FRMS}$ (exemplified in Figure 11 and 12). This is because RoMaP$_{ConKIDDG}$ relies on a non-linear diagnosis model capable of separating scenarios based on complex patterns, which is difficult when using a component-specific HI method based on a single threshold. Combining these aspects, RoMaP$_{ConKIDDG}$ seems to be a superior option on a general basis, but the correct method may depend on the application's requirements. In some scenarios, when FP are acceptable and a low-complexity solution is required, GSIF$_{FRMS}$ and SIF$_{FRMS}$ can be more appropriate.

TABLE 8. Summary of findings based on the experiment. L means low, M medium and H high.

Aspect	GIF$_{CAE}$	SIF$_{FRMS}$	GSIF$_{FRMS}$	RoMaP$_{ConKIDDG}$
Sensitivity	H	H	H	**L**
Prone to give FP	H	M	M	**L**
Prone to give MP	**M**	**M**	**M**	**L**
Prone to FATD	**L**	**L**	**L**	M
Flexibilty	**H**	**H**	**H**	**H**
Complexity	**L**	M	M	H

IX. LIMITATION AND FUTURE WORK

An issue with this study is that it only considered a single component-specific model for fault diagnosis and prognosis. Future research should add more component-level methods to evaluate their performance together. In addition, considering the lack of research on multi-component fault scenarios for rotating machines, it is of great value for future research to suggest alternative frameworks. For example, a hybrid approach between RoMaP and SIF or other combinations could further increase the performance of a predictive maintenance system for rotating machines.

X. CONCLUSION

This study proposes a flexible framework for multi-component fault scenarios of rotating machines using vibration data called RoMaP that leverages the advancements in anomaly detection, fault diagnosis, and RUL prediction. An instance of RoMaP was evaluated based on several scenarios expected in industrial applications and compared against alternative methods based on state-of-the-art research. The result shows that the suggested method was superior on almost all metrics, can successfully handle noise, discrepancies, and multiple fault scenarios, and has a low dependence on parameter selection, unlike the compared methods. This indicates that the suggested framework is suitable for developing robust and accurate methods for monitoring rotating machines, considering multi-component fault scenarios in industrial applications. Despite the promising result, more research should be conducted to optimize the selection of methods for the framework and consider more fault scenarios.

Furthermore, considering the lack of research on methods for multi-component scenarios, future research is encouraged to explore other frameworks to handle this challenge.

REFERENCES

[1] H. Zhou, X. Huang, G. Wen, Z. Lei, S. Dong, P. Zhang, and X. Chen, "Construction of health indicators for condition monitoring of rotating machinery: A review of the research," *Expert Syst. Appl.*, vol. 203, Oct. 2022, Art. no. 117297.

[2] H. Li, Z. Zhang, T. Li, and X. Si, "A review on physics-informed data-driven remaining useful life prediction: Challenges and opportunities," *Mech. Syst. Signal Process.*, vol. 209, Mar. 2024, Art. no. 111120.

[3] D. Neupane, M. R. Bouadjenek, R. Dazeley, and S. Aryal, "Data-driven machinery fault diagnosis: A comprehensive review," *Neurocomputing*, vol. 627, Apr. 2025, Art. no. 129588.

[4] A. Lundström and M. O'Nils, "Factory-based vibration data for bearing-fault detection," *Data*, vol. 8, no. 7, p. 115, Jun. 2023.

[5] S. Gawde, S. Patil, S. Kumar, P. Kamat, K. Kotecha, and A. Abraham, "Multi-fault diagnosis of industrial rotating machines using data-driven approach : A review of two decades of research," *Eng. Appl. Artif. Intell.*, vol. 123, Aug. 2023, Art. no. 106139.

[6] X. Chen, R. Yang, Y. Xue, M. Huang, R. Ferrero, and Z. Wang, "Deep transfer learning for bearing fault diagnosis: A systematic review since 2016," *IEEE Trans. Instrum. Meas.*, vol. 72, pp. 1–21, 2023.

[7] J. J. Montero Jimenez, S. Schwartz, R. Vingerhoeds, B. Grabot, and M. Salaün, "Towards multi-model approaches to predictive maintenance: A systematic literature survey on diagnostics and prognostics," *J. Manuf. Syst.*, vol. 56, pp. 539–557, Jul. 2020.

[8] Y. Zhang, L. Fang, Z. Qi, and H. Deng, "A review of remaining useful life prediction approaches for mechanical equipment," *IEEE Sensors J.*, vol. 23, no. 24, pp. 29991–30006, Dec. 2023.

[9] Y. Ding, P. Ding, X. Zhao, Y. Cao, and M. Jia, "Transfer learning for remaining useful life prediction across operating conditions based on multisource domain adaptation," *IEEE/ASME Trans. Mechatronics*, vol. 27, no. 5, pp. 4143–4152, Oct. 2022.

[10] P. Xia, Y. Huang, P. Li, C. Liu, and L. Shi, "Fault knowledge transfer assisted ensemble method for remaining useful life prediction," *IEEE Trans. Ind. Informat.*, vol. 18, no. 3, pp. 1758–1769, Mar. 2022.
[11] Z. Xu, M. Bashir, Q. Liu, Z. Miao, X. Wang, J. Wang, and N. Ekere, "A novel health indicator for intelligent prediction of rolling bearing remaining useful life based on unsupervised learning model," *Comput. Ind. Eng.*, vol. 176, Feb. 2023, Art. no. 108999.
[12] Y. Deng, S. Du, D. Wang, Y. Shao, and D. Huang, "A calibration-based hybrid transfer learning framework for RUL prediction of rolling bearing across different machines," *IEEE Trans. Instrum. Meas.*, vol. 72, pp. 1–15, 2023.
[13] W. Mao, J. He, and M. J. Zuo, "Predicting remaining useful life of rolling bearings based on deep feature representation and transfer learning," *IEEE Trans. Instrum. Meas.*, vol. 69, no. 4, pp. 1594–1608, Apr. 2020.
[14] J. Zhou, J. Yang, and Y. Qin, "A systematic overview of health indicator construction methods for rotating machinery," *Eng. Appl. Artif. Intell.*, vol. 138, Dec. 2024, Art. no. 109356.
[15] N. Li, Y. Lei, J. Lin, and S. X. Ding, "An improved exponential model for predicting remaining useful life of rolling element bearings," *IEEE Trans. Ind. Electron.*, vol. 62, no. 12, pp. 7762–7773, Dec. 2015.
[16] Q. Ni, J. C. Ji, and K. Feng, "Data-driven prognostic scheme for bearings based on a novel health indicator and gated recurrent unit network," *IEEE Trans. Ind. Informat.*, vol. 19, no. 2, pp. 1301–1311, Feb. 2023.
[17] L. Wen, G. Yang, L. Hu, C. Yang, and K. Feng, "A new unsupervised health index estimation method for bearings early fault detection based on Gaussian mixture model," *Eng. Appl. Artif. Intell.*, vol. 128, Feb. 2024, Art. no. 107562.
[18] M. M. Manjurul Islam, A. E. Prosvirin, and J.-M. Kim, "Data-driven prognostic scheme for rolling-element bearings using a new health index and variants of least-square support vector machines," *Mech. Syst. Signal Process.*, vol. 160, Nov. 2021, Art. no. 107853.
[19] X. Pei, L. Gao, and X. Li, "Remaining useful life prediction of machinery based on performance evaluation and online cross-domain health indicator under unknown working conditions," *J. Manuf. Syst.*, vol. 75, pp. 213–227, Aug. 2024.
[20] Y. Han, M. Xu, X. Sun, X. Ding, X. Chen, and F. Gu, "Gear health monitoring and RUL prediction based on MSB analysis," *IEEE Sensors J.*, vol. 22, no. 5, pp. 4400–4409, Mar. 2022.
[21] J. Zhu, N. Chen, and C. Shen, "A new data-driven transferable remaining useful life prediction approach for bearing under different working conditions," *Mech. Syst. Signal Process.*, vol. 139, May 2020, Art. no. 106602.
[22] Z. Zhao and Y. Jiao, "A fault diagnosis method for rotating machinery based on CNN with mixed information," *IEEE Trans. Ind. Informat.*, vol. 19, no. 8, pp. 9091–9101, Aug. 2023.
[23] Y. Xu, S. Li, X. Yan, J. He, Q. Ni, Y. Sun, and Y. Wang, "Multiattention-based feature aggregation convolutional networks with dual focal loss for fault diagnosis of rotating machinery under data imbalance conditions," *IEEE Trans. Instrum. Meas.*, vol. 73, pp. 1–11, 2024.
[24] D. Wang, K.-L. Tsui, and Q. Miao, "Prognostics and health management: A review of vibration based bearing and gear health indicators," *IEEE Access*, vol. 6, pp. 665–676, 2018.
[25] A. Lundström, M. O'Nils, and F. Z. Qureshi, "Contextual knowledge-informed deep domain generalization for bearing fault diagnosis," *IEEE Access*, vol. 12, pp. 196842–196854, 2024.
[26] H. Zheng, Y. Yang, J. Yin, Y. Li, R. Wang, and M. Xu, "Deep domain generalization combining a priori diagnosis knowledge toward cross-domain fault diagnosis of rolling bearing," *IEEE Trans. Instrum. Meas.*, vol. 70, pp. 1–11, 2021.
[27] Y. Shi, A. Deng, M. Deng, J. Li, M. Xu, S. Zhang, X. Ding, and S. Xu, "Domain transferability-based deep domain generalization method towards actual fault diagnosis scenarios," *IEEE Trans. Ind. Informat.*, vol. 19, no. 6, pp. 7355–7366, Jun. 2022.
[28] B. Wang, Y. Lei, N. Li, and N. Li, "A hybrid prognostics approach for estimating remaining useful life of rolling element bearings," *IEEE Trans. Rel.*, vol. 69, no. 1, pp. 401–412, Mar. 2020.
[29] J. Lee, H. Qiu, and J. Lin. (2007). *Bearing Data Set*. Tech. Services. [Online]. Available: https://www.nasa.gov/content/prognostics-center-of-excellence-data-set-repository
[30] A. Lundstrm and M. O'Nils. (2023). *SCA Bearing Dataset*. [Online]. Available: https://data.mendeley.com/datasets/tdn96mkkpt/1
[31] S. Lee, T. Kim, and T. Kim, "Multi-domain vibration dataset with various bearing types under compound machine fault scenarios," *Data Brief*, vol. 57, Dec. 2024, Art. no. 110940.
[32] W. Gousseau, J. Antoni, F. Girardin, and J. Griffaton, "Analysis of the rolling element bearing data set of the center for intelligent maintenance systems of the University of Cincinnati," in *Proc. CM*, Charenton, France, Oct. 2016, pp. 1–14.

ADAM LYCKSAM received the M.S. degree in industrial engineering and management from Mid Sweden University and the M.S. degree in computer and systems sciences from Stockholm University in 2020. He is currently pursuing the Ph.D. degree in computer engineering with the Department of Computer and Electrical Engineering and employed by SCA. His current research interest includes machine learning solutions for predictive maintenance.

MATTIAS O'NILS received the B.S. degree in electrical engineering from Mid Sweden University, Sundsvall, Sweden, in 1993, and the Licentiate and Ph.D. degrees in electronic systems design from the Royal Institute of Technology, Stockholm, Sweden, in 1996 and 1999, respectively. He is currently a Professor with the Department of Computer and Electrical Engineering and leads a research group in embedded IoT systems at Mid Sweden University. His current research interests include design methods and implementation of embedded DNN-based systems, especially in the implementation of real-time video processing and time series processing systems.

FAISAL Z. QURESHI (Senior Member, IEEE) received the B.Sc. degree in mathematics and physics from Punjab University, Lahore, Pakistan, in 1993, the M.Sc. degree in electronics from Quaid-e-Azam University, Islamabad, Pakistan, in 1995, and the M.Sc. and Ph.D. degrees in computer science from the University of Toronto, Toronto, Canada, in 2000 and 2007, respectively. He is currently a Professor of computer science with the Faculty of Science, Ontario Tech University, where he leads the Visual Computing Laboratory. His research interest includes computer vision. His scientific and engineering interests center on the study of computational models of visual perception to support autonomous, purposeful Behavior in the context of ad hoc networks of smart cameras. He is also active in journal special issues and conference organizations. He is a member of ACM and the Secretary and a member of CIPPRS. He served as the General Co-Chair for the Workshop on Camera Networks and Wide-Area Scene Analysis (co-located with CVPR) from 2011 to 2013. He also served as the Co-Chair for the Computer and Robot Vision (CRV) Conference 2015/2016 meetings.